APPLICATION OF CHARGED MEMBRANES IN ELECTROOSMOTIC PUMPING

Prakhar Prakash, Michael D. Grissom, Christopher D. Rahn, and Andrew L. Zydney
The Pennsylvania State University, University Park, PA, USA

Introduction

Electroosmosis refers to the bulk fluid motion that develops when a voltage is applied across an electrolyte solution contained in a channel that is bounded by electrically charged surfaces. The charged surface generates a region containing a high (excess) concentration of counterions, referred to as the electrical double layer, with the net fluid flow in the channel arising from the motion of the ions within the double layer in response to the applied voltage.

Electroosmotic pumps have been examined for a wide range of applications, including liquid chromatography [1, 2], lab-on-a-chip systems [3, 4, 5], cooling of microelectronic equipment [6], drug delivery [7], and actuation devices [8]. Electroosmotic pumps are attractive because they involve no moving parts, can achieve relatively high pressures, and provide a constant non-pulsatile flow. A variety of porous materials have been used to generate the charged channels, including porous glass frits [9]; open channels [10] and capillary columns packed with spherical beads or porous silica spheres [1]. However, almost all of these applications have focused on systems that require very low flow rates, often in the range of nL/s for many lab-on-a-chip systems. More recently, Norman et al. [11-13] described the development of an electrochemical pumping system using cation-selective ionomer (Nafion 117) membranes. An iodide / triiodide redox electrolyte was used, formed by a solution of tetraalkylammonium iodide in dimethylformamide. The use of this redox couple allowed operation at significant currents without gas generation since there was no electrolysis. The pump was able to generate pressures as high as 2 MPa [13], although the maximum reported flow rate was less than 1 µL/s [11],

The overall goal of this work was to develop an effective electroosmotic pump to drive a high mechanical advantage actuator capable of generating large block stresses and large strains suitable for the control of airplane wings, underwater control fins, or morphing surfaces [14]. Electroosmotic pumps are attractive since they can provide a voltage-regulated flow and pressure with very quiet operation, which is of particular interest for military applications. However, the pumps must be able to generate pressures in excess of 0.1 MPa (14.5 psi) while providing volumetric flow rates on the order of 0.1 mL/s, performance characteristics that are quite different than those encountered in most previous applications of electroosmotic pumping. Initial experimental work was focused on identifying a

membrane with appropriate surface charge and pore size for this application. Subsequent efforts were focused on the design of a multi-stage electroosmotic pump that was capable of providing the desired flow rates and pressures.

Theoretical Background

The magnitude of the electroosmotic flow is determined by the surface charge, pore size, porosity, and thickness of the porous medium. Most theoretical models of electroosmotic flow are based on an analysis of flow through a parallel array of uniform cylindrical pores of radius a [15-18]. The fluid flow rate is evaluated by solving the Navier-Stokes equations accounting for the electrical stresses:

$$-\frac{dP}{dz} + \frac{\mu}{r}\frac{\partial}{\partial r}\left(r\frac{\partial v_z}{\partial r}\right) + E_z\rho_e = 0 \tag{1}$$

where dP/dz is the pressure gradient, μ is the fluid viscosity, v_z is the axial velocity at radial position r, and E_z is the axial electric field. The local volumetric charge density, ρ_e, is related to the electrostatic potential, ϕ, using Poisson's equation:

$$\frac{1}{r}\frac{\partial}{\partial r}\left(r\frac{\partial \phi}{\partial r}\right) = -\frac{\rho_e}{\varepsilon} = -\frac{F}{\varepsilon}\sum_i z_i c_i \tag{2}$$

where ε is the permittivity of the medium, F is Faraday's constant, and z_i and c_i are the valence and molar concentration of the different ionic species. The ion concentrations in the pore are described by a Boltzmann distribution:

$$c_i = c_o \exp -\frac{z_i F\phi}{RT} \tag{3}$$

Equation (2) is substituted into Equation (1) which is then integrated twice with respect to r giving:

$$Q = 2\pi \int_0^a r v_z dr = -E_z\frac{\pi\varepsilon}{\mu}\int_0^a r^2\frac{\partial \phi}{\partial r}dr - \frac{\pi a^4}{8\mu}\frac{dP}{dz} \tag{4}$$

Equation (4) is identical to the result presented previously by Newman [18]. The initial (maximum) flow rate (Q_{max}) is evaluated directly from Equation (4) by setting the pressure gradient (dP/dz) equal to zero while the maximum pressure gradient is determined by setting $Q = 0$. The integral involving the gradient of the electrical potential was evaluated by numerical solution of the Poisson-Boltzmann equation (Equations 2 and 3). The boundary value problem was solved in MATLAB using algorithm bvp4c, which is a finite difference code that implements the three-stage Lobatto IIIa collocation formula that provides a C1-continuous solution that is fourth order accurate. Mesh selection and error control are based on the residual of the continuous solution.

The ion flux through the charged media is evaluated from the sum of the electromigration and advection fluxes:

$$N_{iz} = z_i u_i F c_i E_z + c_i v_z \tag{5}$$

where u_i is the ionic mobility of species i. The net current is thus given as:

$$I = 2\pi \int_0^a rF \sum z_i N_i dr = 2\pi E_z \int_0^a r\kappa dr + 2\pi E_z \frac{\varepsilon^2}{\mu} \int_0^a r \left(\frac{\partial \phi}{\partial r}\right)^2 dr + \frac{dP}{dz} \frac{\pi\varepsilon}{\mu} \int_0^a r^2 \frac{\partial \phi}{\partial r} dr \tag{6}$$

where κ is the conductivity of the electrolyte solution. The required integrals in Eq. (6) were evaluated in MATLAB using the previously developed solution for the electrical potential.

Materials and Methods

Electroosmotic flow measurements were obtained using the apparatus shown in **Figures 1**. The device was machined from polycarbonate with the charged membrane supported between two 350 mL chambers. Electroosmotic pumps were constructed using several inorganic membranes made of 99.99% silica or alumina. Silica membranes (>99.99% silica) were obtained from Andrews Glass Company (Vineland, NJ) and Advanced Glass and Ceramics (Holden, MA). Alumina membranes (>99.99% alumina) were obtained from Coorstek (Golden, CO). Data were obtained with KCl solutions prepared in deionized distilled water.

Results and Analysis

The zeta potential for each membrane was determined from the slope of the streaming potential versus transmembrane pressure data using the Helmholtz-Smoluchowski equation [18] and following the method developed by Burns and Zydney [19]:

$$\frac{dV}{d\Delta P} = \frac{\varepsilon_o \varepsilon_r}{\mu\kappa} \varsigma \tag{7}$$

The zeta potential for the silica membrane with 0.6 µm pore size was -0.063 ± 0.001 V, while that for the silica membrane with 0.3 µm pore size was only –0.006 V. This difference is likely due to different surface treatments used in the manufacture of the porous silica which result in significant differences in the number of charged groups on the final silica membrane. The zeta potential for both the silica and alumina membranes appeared to be inversely correlated with the membrane pore radius, even though the pores in these membranes were much larger than the double layer thickness (Debye length) under these experimental conditions.
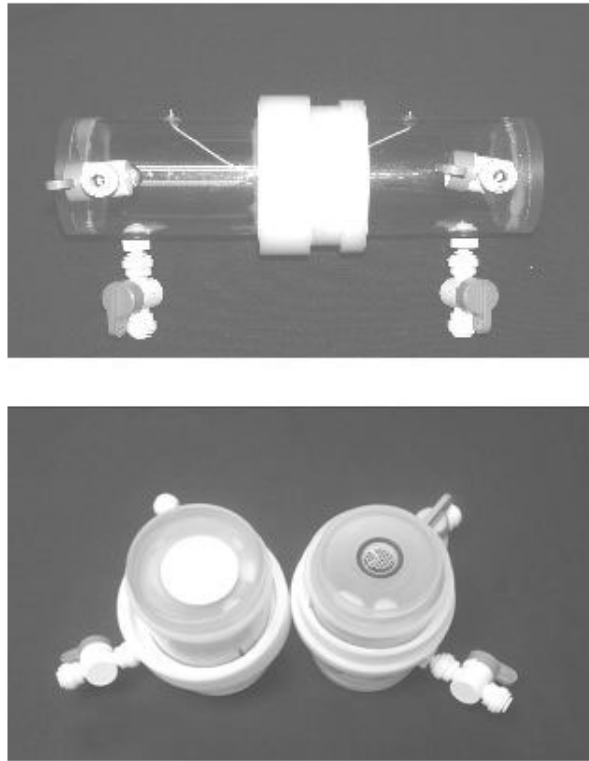
Figure 1: Small scale electroosmotic pump. Exploded view (lower panel) shows membrane and O-ring.

Electroosmotic Pumping:

Initial pumping experiments were performed with the silica membrane obtained from Andrews Glass which had a zeta potential of -0.060 mV. Results for the maximum flow rate (Q_{max}), the maximum current (I_{max}), and the maximum pressure (P_{max}) are shown in **Figures 2a, b, and c** as function of the applied voltage. The maximum flow rate and current were both evaluated shortly after application of the applied voltage (typically within 2 min), i.e., under conditions where the pressure drop across the silica membrane was negligible. The values for the maximum flow rate have been corrected to account for the effects of hydrogen evolution at the cathode, with the volumetric contribution from hydrogen generation estimated assuming ideal gas behavior as:
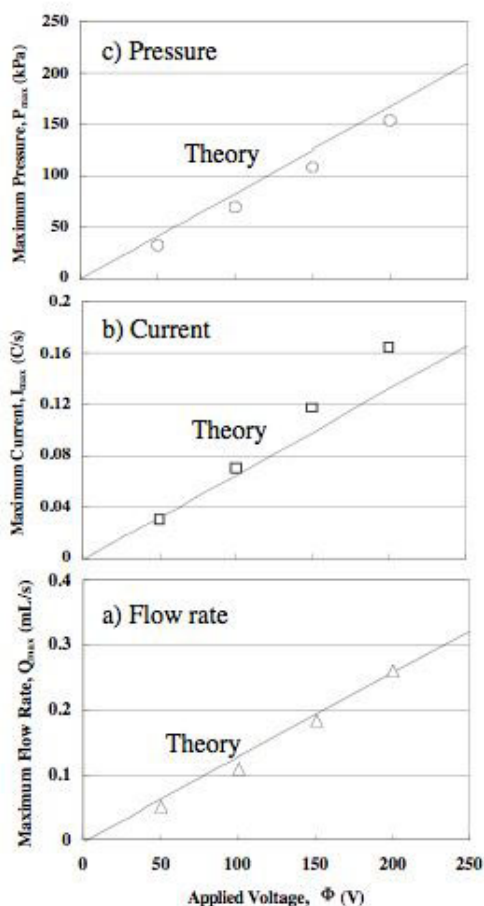
$$Q_{H_2} = \frac{IkT}{2eP} \tag{8}$$

Figure 2: Electroosmotic pumping performance for silica membrane with 0.6 μm pore radius: (a) maximum flow rate, (b) maximum current, and (c) maximum pressure.

where P is the pressure in the cathode chamber, k is the Boltzmann constant, and T is the absolute temperature. The contribution from hydrogen evolution was typically less than 10% of the measured volumetric flow rate. The maximum flow rate at 200 V was 0.26 mL/s, corresponding to a linear velocity of 1.5 x 10^{-3} m/s based on the membrane cross-sectional area. The maximum pressure (0.16 MPa at 200 V) was determined by clamping the exit flow line, with the pressure evaluated after the system had stabilized (i.e., after the volumetric flow rate had dropped to a negligible value). The solid lines in **Figures 2a – c** are model calculations developed from Equations 1 to 8 with the model in good agreement with the data.

Experimental data for the different alumina and silica membranes are plotted as a function of the membrane pore radius in **Figure 3**. The y-axis is the ratio of the maximum flow rate to the maximum pressure, with this ratio being independent of both the applied voltage and the membrane zeta potential. The solid curve is the model calculation for Q_{max}/P_{max}, which is in excellent agreement with the experimental data. Decreasing the pore radius causes a significant

increase in the maximum attainable pressure with relatively little change in the maximum flow rate, allowing one to fine tune the performance of the electoosmotic pump to meet specific design criteria.
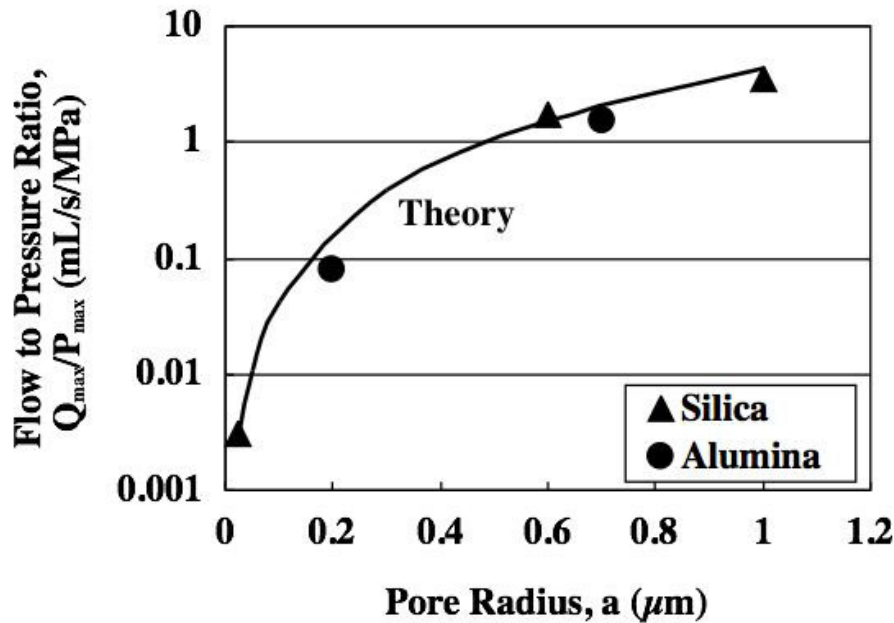

Figure 3: Ratio of maximum flow rate to maximum pressure as a function of the membrane pore size. Data obtained at pH 10.3 and 2 mM ionic strength.

Pump scale-up: Design and performance

The membranes examined in the previous section provide reasonable flow rates (> 0.25 mL/s) and pressures (> 0.1 MPa); however, some applications of the high mechanical advantage actuators require a significantly higher combination of pressure and flow. A straightforward method for extending the capabilities of the electroosmotic pump is to connect several units in parallel to produce higher flow rates or in series to produce higher pressures. When operated in parallel, the volumetric flow from each pump will be additive, which was confirmed from experiments performed with 2 separate pumping units using 0.6 µm pore size, 34 mm diameter silica membranes. The total flow rate for this 2-pump parallel system was nearly 4.1 mL/s at 370 V while the maximum pressure remained above 0.1 MPa. A multistage series pump using capillaries packed with porous silica particles has been described by Chen et al. [20]. A novel compact modular design was developed in this work that allowed large

numbers of membranes to be placed in a single device (Figure 4). The key to the performance of these multi-stage pumps was maintaining a large electrical resistance between the stages while minimizing the hydrodynamic (flow) resistance. This was accomplished using a spiral inset that provided minimal resistance to flow while giving a large effective path length between the electrodes. A 10-membrane device of this configuration could provide pressures above 1.6 MPa with a total volume less than 200 mL
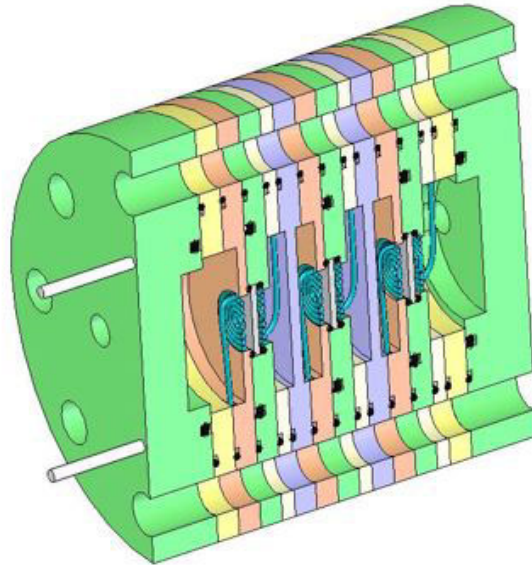

Figure 4: Cross-sectional view of a 3-membrane electroosmotic pump with modular stages in series.

Discussion

The results obtained in this study demonstrate that it is possible to develop electroosmotic pumps capable of providing relatively high pressures (> 0.1 MPa) and moderate flow rates (> 0.1 mL/s) that are suitable for the development of high mechanical advantage actuators. The performance characteristics of the electroosmotic pumps could be optimized for specific applications through the choice of membrane properties, electrolyte concentration, and applied voltage. Further improvements in performance were achieved using multiple membranes in parallel arrangement to generate high flow rates or in series to generate high block pressures. A novel compact modular design was developed that allowed large numbers of membranes to These nove_l pumps can be scaled up (or down) to meet the flow and pressure requirements for a wide range of applications in

which quiet operation, absence of moving parts, and / or minimal pulsatility are of particular benefit.

Acknowledgements

REFERENCES

[1]   L.X. Chen, J.P. Ma, Y.F. Guan, Study of an electroosmotic pump for liquid delivery and its application in column liquid chromatography, J. Chromat. A, 1028 (2004) 219 – 226.

[2] L. Chen, J. Ma, Y. Guan, An electroosmotic pump for packed capillary liquid chromatography, Microchemical Journal, 75(1) 2003 15-21.

[3]   J.P. Kutter, S.C. Jacobson, J.M. Ramsey, Integrated microchip device with electrokinetically controlled solvent mixing for isocratic and gradient elution in micellar electrokinetic chromatography, Anal. Chem., 69 (1997) 5165 – 5171.

[4]   P.C.H. Li, D.J. Harrison, Transport, manipulation, and reaction of biological cells on-chip using electrokinetic effects, Anal. Chem., 69 (1997) 1564 – 1568.

[5]   A.G. Hadd, D.E. Raymond, J.W. Halliwell, S.C. Jacobson, J.M. Ramsey, Microchip device for performing enzyme assays, Anal. Chem., 69 (1997) 3407–3412.

[6]   L. Jiang, J. Mikkelsen, J.-M. Koo, D. Huber, S. Yao, L. Zhang, P. Zhou, J.G. Maveety, R. Prasher, J.G. Santiago, T.W. Kenny, K.E. Goodson, Closed-loop electroosmotic microchannel cooling system for VLSI circuits, IEEE Trans. Comp. Packag. Manufact. Tech., 25 (2002) 347 – 355.

[7]   M.J. Pikal, The role of electroosmotic flow in transdermal iontophoresis, Adv. Drug Deliv. Rev., 46 (2001) 281 – 305.

[8]   P.H. Paul and D.J Rakestraw, Electrokinetic high pressure hydraulic system, U.S. Patent, 6,019,882 (2000).

[9] S.L. Zeng, C.H. Chen, J.C. Mikkelsen, J.G. Santiago., Fabrication and characterization of electroosmotic micropumps, Sens. Actuators B, 79 (2001) 107-114.

[10] I.M. Lazar, B.L. Karger, Multiple open-channel pumping system for microfluid sample handling, Anal. Chem., 74 (2002) 6259 – 6268.

[11] M. Norman, R.D. Noble, C.A. Koval, Electrochemical pumping of DMF electrolyte solutions across membranes, *J. Electrochem. Soc.*, 151 (2004) E364 - E369.

[12] M.A. Norman, C.E. Evans, A.R. Fuoco, R.D. Noble, C.A. Koval, Characterization of a 2embrane-based, electrochemically driven pumping system using aqueous electrolyte solutions, *Anal. Chem.*, 77 (2005) 6374 – 6380.

[13] C.E. Evans, R.D. Noble, C.A. Koval, A nonmechanical, membrane-based liquid pressurization system, *Ind. Eng. Chem. Res.*, 45 (2006) 472 – 475.

[14] M.K. Philen, Y. Shan, P. Prakash, K.W. Wang, C.D. Rahn, A.L. Zydney, C.E Bakis, Fibrillar Network Adaptive Structure with Ion Transport Actuation., J. Intelligent Material Systems and Structures (JIMSS), (in press).

[15] S. Yao, D.E. Hertzog, S. Zeng, J.C. Mikkelsen, J.G. Santiago, Porous glass electroosmotic pumps: design and experiments, J. Coll. Interf. Sci., 268 (2003) 143 – 153.

[16] C.L. Rice, R.J. Whitehead, Electrokinetic flow in a narrow cylindrical capillary, J. Phys. Chem., 69 (1965) 4017 – 4035.

[17] S. Yao, J.G. Santiago, Porous glass electroosmotic pumps: theory, J. Colloid Interface Sci. 268 (2003) 133-142.

[18] J.S. Newman, <u>Electrochemical Systems</u>, 2nd Edition, Prentice Hall, Englewood Cliffs, MJ (1991).

[19] D.B. Burns, A.L. Zydney, Buffer effects on the Zeta potential of ultrafiltration membranes, J. Membr. Sci., 172 (2000), 39 - 48.

[20] L. Chen, H. Wang, J. Ma, C. Wang, Y. Guan, Fabrication and characterization of a multi-stage electroosmotic pump for liquid delivery, Sens. Actuators B, 104 (2005) 117 – 123.